World Academy of Science, Engineering and Technology
International Journal of Energy and Power Engineering
Vol:13, No:5, 2019

A Single Switch High Step-Up DC/DC Converter with Zero Current Switching Condition

Rahil Samani, Saeed Soleimani, Ehsan Adib, Majid Pahlevani

Abstract**—**This paper presents an inverting high step-up DC/DC converter. Basically, this high step-up DC/DC converter is an appealing interface for solar applications. The proposed topology takes advantage of using coupled inductors. Due to the leakage inductances of these coupled inductors, the power MOSFET has the zero current switching (ZCS) condition, which results in decreased switching losses. This will substantially improve the overall efficiency of the power converter. Furthermore, employing coupled inductors has led to a higher voltage gain. Theoretical analysis and experimental results of a 100W 20V/220V prototype are presented to verify the superior performance of the proposed DC/DC converter.

Keywords**—**Coupled inductors, high step-up DC/DC converter, zero-current switching, cuk converter, sepic converter.

I. Introduction

THE nonstop pace of technology growth in recent decades has caused rapid growing demand for reliable energy sources all around the world. Global warming and other environmental consequences have drawn more attention to renewable energy resources like photovoltaic (PV) cells. PV array application has become popular in many fields like power generation for grid, standalone off-grid power stations, battery chargers, and etc. a general diagram of a two-stage power conditioning system for a grid connected PV system is illustrates in Fig. 1. Despite their clean power generation and long term working life, there are some aspects which need to be modified in practice, the regular output voltage of solar panels is about 20-30V that needs to be increased in order to inject power to the grid. Also, unstable characteristics of solar panels demand Maximum Power Point Tracking (MPPT) algorithm and proper DC/DC or DC/AC converter to achieve stable and regulated output power [1]-[5].

The traditional voltage-boosting non-isolated converters (e.g. boost converter and buck-boost converter) can theoretically show very high voltage conversion gain in high duty cycles but extreme large conduction losses affects both the efficiency and conversion ratio. Thus, their voltage gains would not be high enough, which is a serious limit. Furthermore, the high output voltage requires high voltage semiconductor devices. Consequently, a high-voltage switch would increase the switching loss and also high-voltage diodes reduce the efficiency due to serious reverse recovery issues. Also, cascade connection of aforementioned converters results in high gain but power is processed twice [6]-[10].

R. Samani is with the Department of Electrical and Computer Engineering, University of Calgary, Calgary, AB, Canada (e-mail: rahil.ghatrehsamani@ucalgary.ca).
S. Soleimani and E. Adib are with the Department of Electrical and Computer Engineering, Isfahan University of Technology, Isfahan, Iran.
M. Pahlevani is with the Department of Electrical and Computer Engineering, University of Calgary, Calgary, AB, Canada.

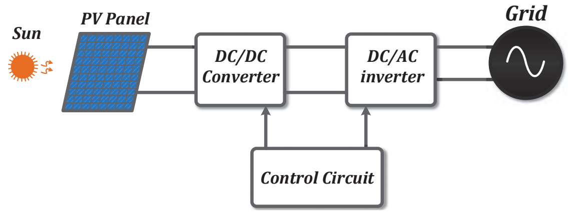

Fig. 1 Block Diagram of Grid-Connected PV Systems

The main aim in designing a high step-up converter is to efficiently convert power while using minimum components to simplify the control method. So far, many different kinds of high step-up techniques have been applied such as coupled inductors and switched capacitors, [11]-[13]. Topologies based on coupled inductor suffer from stored energy in the leakage inductor which causes a voltage spike on main power MOSFET leading to higher power dissipation. Hence, active or passive clamp circuits are required. Transformer based topologies can give a very high output gain by adjusting the turn ratio. Serious draw-backs are increased number of controlled switches and large leakage inductance of transformer [14]-[21]. The converter presented in [22], considers a way to decrease the turn-off loss of the switch which enhances the efficiency of the converter and reducing current ripple while presenting a high boosting gain.

Some earlier high step-up circuits employ interleaved structures in order to reduce switch currents and increase the transferred power. However, two switches are required. The main objective of this work is to develop a high-efficiency high step-up topology as an interface for renewable energy resources. Such structures which combine coupled inductors and voltage-doublers are compatible with other topologies, especially in their voltage gain [23]-[25]. In [26], a single switch high step-up converter employing voltage-doubler on Sepic topology is presented. Although it has equal number of components to the proposed converter, the voltage gain of the proposed converter is noticeably higher which is due to the utilization of coupled inductors.

The main obtained advantages of the proposed converter are low operating duty cycles, low switch voltage stress, low size and cost of the circuit and high voltage conversion ratio. In the proposed converter, the switch voltage is inherently clamped and therefore, the energy of the leakage inductance of coupled inductors, which is usually problematic in high step-up converters, is absorbed and transferred to the output.

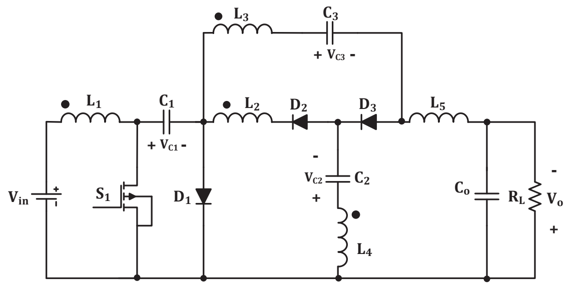

Fig. 2 The Proposed High Step-Up DC/DC Converter

In the proposed topology, the leakage inductor of the coupled inductors provides ZCS for the power MOSFET in order to reduce switching and reverse recovery losses. These features verify the high efficiency of the converter.

II. Configuration of the Proposed Converter

In this section a high step-up DC/DC converter is introduced. The topology is derived from the Cuk converter. This circuitry takes advantage of utilizing coupled inductors and switch capacitor techniques in order to boost the output voltage. Coupled inductors provide the capability of integrating the magnetic structure, which significantly reduces the size and the cost of the converter. The proposed converter consists of a single low voltage power MOSFET, three diodes, four capacitors, four coupled inductors and an output inductor. Power MOSFET S_1 and diode D_2 conduct simultaneously, whereas diodes D_3 and D_1 conduct in a complementary manner. When the power MOSFET turns on, inductor L_1 stores the input energy. This stored energy is discharged in the circuit when the power MOSFET turns off. In order to simplify the analysis, the following assumptions are considered:

- All components are assumed ideal
- Converter is in its steady state
- Capacitors and the output inductor are large enough to have constant voltages and current, respectively

Fig. 3 illustrates the steady-state qualitative waveforms of diode currents D_1, D_2, and D_3, power MOSFET S_1, and capacitors C_1, C_2, and C_3. Operating in continuous conduction mode (CCM), the converter has three operation modes in each switching cycle, which are explained in the following:

1) Mode I ($t_0 \leq t < t_1$): Fig. 4 (a) shows the equivalent circuit during this time interval. Due to the leakage inductance of the of coupled inductors, power MOSFET S_1 and diode D_2 turn on under ZCS condition (diodes D_1 and D_3 are off). In this state, the input voltage is directly applied to inductor L_1. Therefore, the magnetizing input inductor is being charged and its current (i_{L_m}) would increase linearly. Furthermore, a coefficient of the input voltage is induced on each coupled inductor, which is due to the coupling between inductors L_1, L_2, L_3, and L_4. In this mode, capacitors C_1 and C_3 are discharging

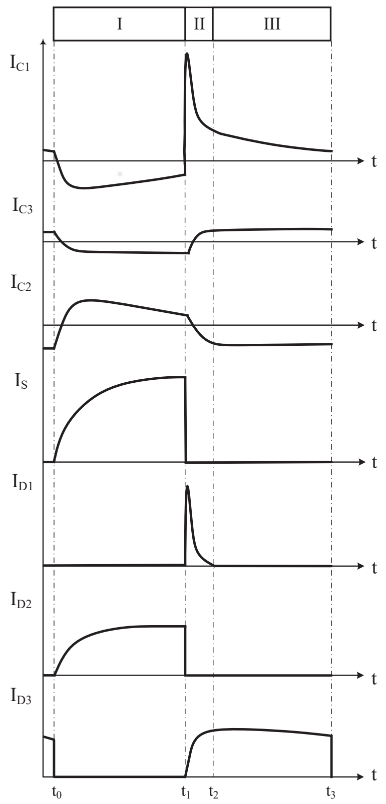

Fig. 3 Operation Modes of the Proposed converter: (a) Mode I, (b) Mode II, (c) Mode III

and capacitor C_2 is charging. Mathematical equations of this mode are explained in the following:

$$V_{L_1} = V_{in} \tag{1}$$

$$V_{L_2} = V_{L_3} = V_{L_4} = nV_{in} \tag{2}$$

$$n = \frac{N_2}{N_1} \tag{3}$$

$$V_{C_2} - V_{C_1} = 2nV_{in} \tag{4}$$

where N_1 and N_2 are numbers of windings in the primary and secondary sides of the inductor. Inductors L_3 and L_4 have the same turn ratios as the inductor L_2. This mode lasts until power MOSFET S_1 turns off.

2) Mode II ($t_1 \leq t < t_2$): Fig. 4 (b) shows the equivalent circuit during this time interval. The power MOSFET S_1 and the diode D_2 turn off. Consequently, diodes D_1 and D_3 turn on. In this mode, the stored energy in the magnetizing inductor L_m is transferred to the capacitor C_1. Moreover, the other part of the energy of the magnetizing inductor L_m is transferred through the coupling between the inductors L_1, L_3 and L_4, which charges the capacitor C_3 and discharges the capacitor C_2. Consequently, the current of the magnetizing inductor (i_{L_m}) decreases. Equations in this mode are as following:

$$V_{L_1} = V_{in} - V_{C_1} \tag{5}$$

$$V_{L_2} = V_{L_3} = V_{L_4} = nV_{in} - nV_{C_1} \tag{6}$$

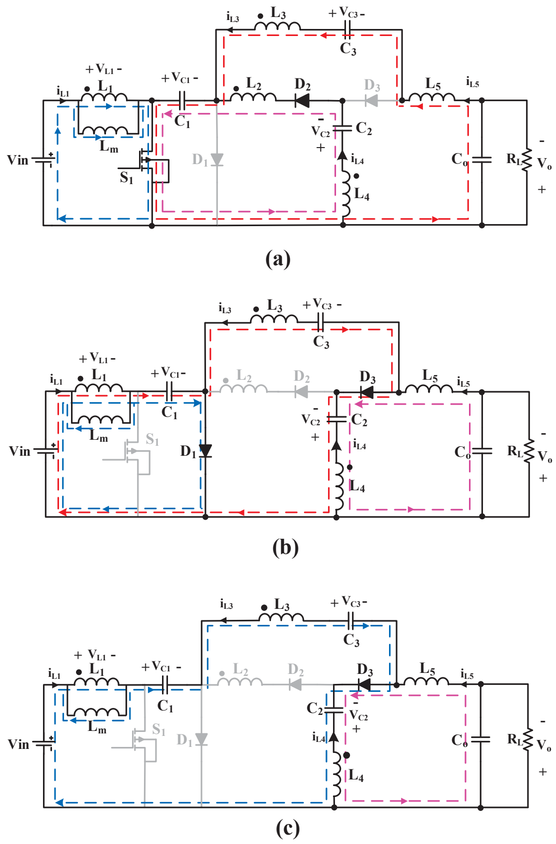

Fig. 4 Steady state waveforms of the proposed converter

$$V_{C_2} - V_{C_3} + 2nV_{C_1} = 2nV_{in} \tag{7}$$

3) Mode III ($t_2 \leq t < t_3$): Fig. 4 (c) shows the equivalent circuit during this time interval. As the voltage of the capacitor C_1 (V_{C_1}) increases, the current through this capacitor decreases. When it reaches the current I_{C_3}, the current through the diode D_1 reaches zero. Therefore, the diode D_1 stops conducting under ZCS condition. Since the diode D_1 is off, in the next switching cycle the power MOSFET is turned on under ZCS. In this situation, the reverse recovery losses are eliminated.

$$V_{in} = V_{L_1} + V_{C_1} + V_{L_3} + V_{C_3} - V_{C_2} + V_{L_4} \tag{8}$$

By substituting (2), (3) and (7) in the above equation:

$$V_{L_1} = V_{in} - V_{C_1} \tag{9}$$

Equation (9) is equals to (5). This indicates that the voltage dropped on the inductor L_1 in the third mode is equal to the voltage dropped on the inductor L_1 in the second mode.

III. Operating Principle of the Proposed Converter

In this section operating principles of the proposed converter is analyzed. In order to acquire the converter voltage gain, the volt-second-balance (VSB) equations of the input and the output inductors should be written.

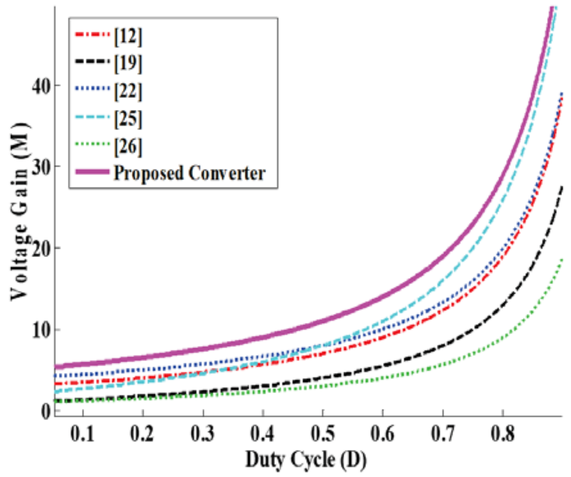

Fig. 5 Comparisons of the Voltage Gain versus Duty Cycle in the Proposed Converter and Conventional High Step-Up Converters

From (1), (5), and (9):

$$\int_{t_0}^{t_3} V_{L_1} dt = DV_{in} + (1-D)(V_{in} - V_{C_1}) = 0 \tag{10}$$

$$\int_{t_0}^{t_3} V_{L_2} dt = D(V_o + nV_{in} - V_{C_2} - V_{C_3}) + \tag{11}$$

$$(1-D)(V_o + nV_{in} - V_{C_2} - nV_{C_1}) = 0$$

From (10), (11):

$$V_{C_1} = \frac{V_{in}}{(1-D)T} \tag{12}$$

$$V_{C_2} + DV_{C_3} = V_o \tag{13}$$

Eventually, from (4), (7), and (13), the high step-up voltage gain is derived as:

$$M = \frac{V_o}{V_{in}} = \frac{2n + 1 + D}{1 - D} \tag{14}$$

Considering the current through the magnetizing inductor L_m and the current-second-balance (CSB) equations in capacitors C_2 and C_3, it can be achieved that:

$$I_{in_{ave}} = D(I_{L_m} + nI_{C_2} + nI_{C_3}) + (1-D)(I_{L_m} - nI'_{C_2} - nI'_{C_3}) \tag{15}$$

$$DT(I_{C_2}) = (1-D)T(I'_{C_2}) \tag{16}$$

$$DT(I_{C_2}) = (1-D)T(I'_{C_2}) \tag{17}$$

where I_{C_3} and I_{C_2} represent the charging currents through the capacitors C_3 and C_2, respectively. Likewise, I'_{C_3} and I'_{C_2} represent the discharging currents through the capacitors. According to the equations in the operation modes:

$$I_{C_3} = I_o \tag{18}$$

Since the converter is assumed ideal:

$$I_o = \frac{P_{in}}{V_{in}} \tag{19}$$

TABLE I
SPECIFICATIONS OF THE PROPOSED CONVERTER

Parameter	Value
Input Inductor L_1	$100\mu H$
Coupled Inductors L_2, L_3, L_4	$400\mu H$
Output Inductor L_5	$3mH$
Diodes D_2, D_3	MUR860
Diode D_1	MUR1560
Capacitor C_1	$2.2\mu F$
Capacitor C_2	$1.5\mu F$
Capacitor C_3	$1\mu F$
Capacitor C_o	$4.7\mu F$
Power Switch S_1	IRF540
Turn Ratio ($n = \frac{N_2}{N_1}$)	2
Input Voltage V_{in}	20 V
Output Power P_o	100 W

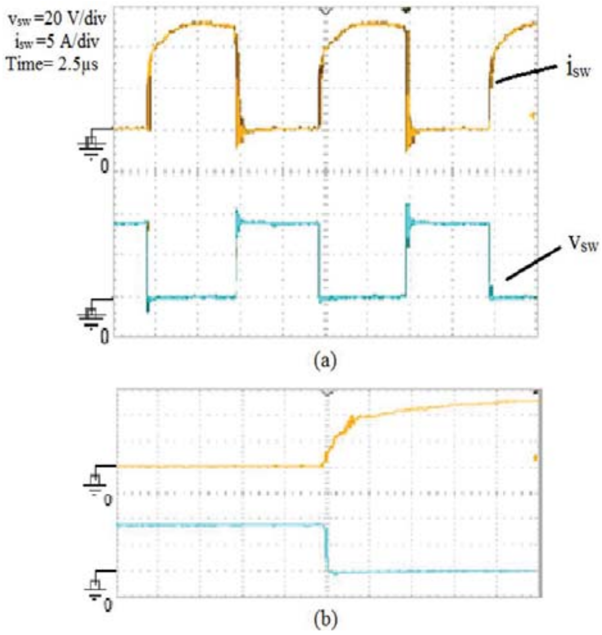

Fig. 6 (a) Voltage and Current Waveforms of the Power MOSFET S_1 and (b) the Smooth Transition of the Power Switch Turn-On

And also from the CSB equation for the capacitor C_1:

$$D(nI_{C_2} + nI_{C_3}) = (1-D)(I_{L_m} - nI'_{C_2} - nI'_{C_2}) \tag{20}$$

The charging and discharging currents of these three capacitors are calculated from (14)-(20), which is used to determine the capacitances. Considering the basic power (20), it is obtained that:

$$P_{in} = (I_{in_{ave}}).V_{in} \tag{21}$$

From (15)-(18):

$$I_{L_m} = \frac{P_{in}}{V_{in}} \tag{22}$$

From (16)-(20):

$$I_{C_2} = \frac{(1-D)P_{in}}{2nDV_{in}} - \frac{P_{in}}{V_o} \tag{23}$$

The charging current through the capacitor C_1 can be calculated based on (20) and (23). In Fig. 6, a comparison between the voltage gains of the proposed converter and other converters in [10], [17], [19], [20], [22], and [23] is depicted. This comparison verifies the superior performance of the proposed converter.

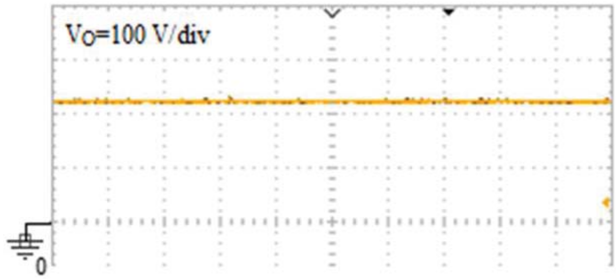

Fig. 7 The Output Voltage of the Prototype Circuit

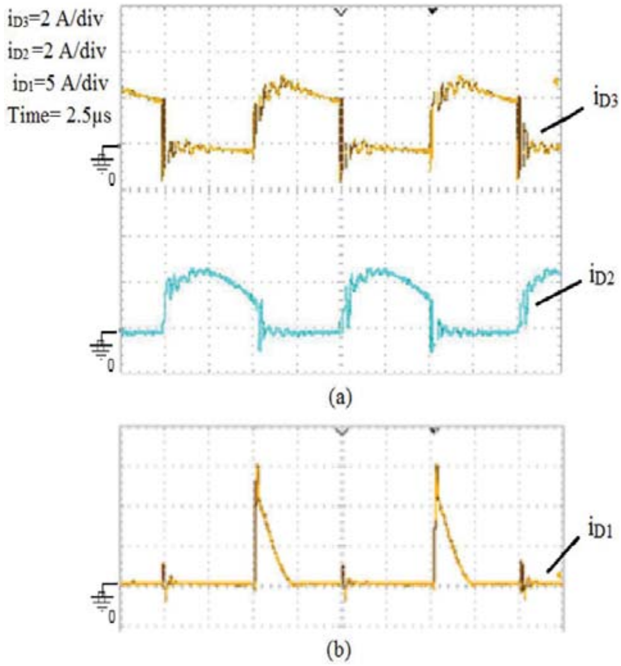

Fig. 8 Current Waveforms of Diodes (a) D_1, D_2 and (b) D_3

IV. EXPERIMENTAL RESULTS

In order to verify the analysis of the proposed converter, a 100W prototype is implemented. The input voltage and switching frequency are 20V and 100 KHz, respectively. This circuit has been designed to have a 220V output voltage.

The turn ratio of the coupled inductors is 2. According to Eq. (14), the converter is designed to work with duty cycle of about 50%, which results in a voltage gain of 11. Specifications of the prototype circuit are listed in Table I. Fig. 6 (a) shows the voltage and current waveforms of the power MOSFET S_1. According to this figure, the power MOSFET S_1 turns on with ZCS condition. In Fig. 6 (b), the smooth transition of the power MOSFET turn-on is shown. Fig. 7 shows the inverted output voltage of the proposed converter. The output voltage is about 220V, which verifies the theoretical analysis. Fig. 8 (a) depicts the currents i_{D_2} and i_{D_3} and Fig. 8 (b) shows the current i_{D_1}.

V. Conclusion

This paper proposed a high step-up DC/DC converter with an inverted output polarity voltages. The improved gain makes this converter suitable for solar applications. Furthermore, merging this topology with a non-inverting converter will provide a bipolar structure for AC-module applications. The ZCS condition of the power MOSFET improves the overall efficiency of the proposed DC/DC converter. In addition, using a single switch with low on-state resistance has improved the cost, efficiency, and simplicity of the converter. There are no voltage spikes across the power MOSFET of this converter since the circuit clamps the voltage inherently and the leakage inductance energy of the coupled inductors is recovered. The experimental results of the prototype completely verify the theoretical analysis and the feasibility of the circuit.

References

[1] A. Ajami, H. Ardi and A. Farakhor, “A Novel High Step-up DC/DC Converter Based on Integrating Coupled Inductor and Switched-Capacitor Techniques for Renewable Energy Applications,” in IEEE Transactions on Power Electronics, vol. 30, no. 8, pp. 4255-4263, Aug. 2015.

[2] M. Amirbande, K. Yari, M. Forouzesh and A. Baghramian, “A novel single switch high gain DC-DC converter employing coupled inductor and diode capacitor,” 2016 7th Power Electronics and Drive Systems Technologies Conference (PEDSTC), Tehran, 2016, pp. 159-164.

[3] J. M. Carrasco et al., “Power-Electronic Systems for the Grid Integration of Renewable Energy Sources: A Survey,” in IEEE Transactions on Industrial Electronics, vol. 53, no. 4, pp. 1002-1016, June 2006.

[4] M. C. Tanca V. and I. Barbi, “A high step-up gain DC-DC converter based on the stacking of three conventional buck boost DC-DC converters,” XI Brazilian Power Electronics Conference, Praiamar, 2011, pp. 196-200.

[5] S. Changchien, T. Liang, J. Chen and L. Yang, “Novel High Step-Up DC–DC Converter for Fuel Cell Energy Conversion System,” in IEEE Transactions on Industrial Electronics, vol. 57, no. 6, pp. 2007-2017, June 2010.

[6] K. I. Hwu and Y. T. Yau, “High Step-Up Converter Based on Coupling Inductor and Bootstrap Capacitors With Active Clamping,” in IEEE Transactions on Power Electronics, vol. 29, no. 6, pp. 2655-2660, June 2014.

[7] K. Park, G. Moon and M. Youn, “Nonisolated High Step-up Boost Converter Integrated With Sepic Converter,” in IEEE Transactions on Power Electronics, vol. 25, no. 9, pp. 2266-2275, Sept. 2010.

[8] C. Leu and M. Li, “A Novel Current-Fed Boost Converter With Ripple Reduction for High-Voltage Conversion Applications,” in IEEE Transactions on Industrial Electronics, vol. 57, no. 6, pp. 2018-2023, June 2010.

[9] D. Gao, Z. Jin, J. Liu, and M. Ouyang, “An interleaved step-up/step-down converter for fuel cell vehicle applications,” Int. J. Hydrogen Energy, vol. 41, no. 47, pp. 22422–22432, 2016.

[10] T. Nouri, S. H. Hosseini, E. Babaei, and J. Ebrahimi, “A non-isolated three-phase high step-up DC–DC converter suitable for renewable energy systems,” Electr. Power Syst. Res., vol. 140, pp. 209–224, 2016.

[11] N. Vazquez, L. Estrada, C. Hernandez and E. Rodriguez, “The Tapped-Inductor Boost Converter,” 2007 IEEE International Symposium on Industrial Electronics, Vigo, 2007, pp. 538-543.

[12] A. A. Fardoun and E. H. Ismail, “Ultra Step-Up DC–DC Converter With Reduced Switch Stress,” in IEEE Transactions on Industry Applications, vol. 46, no. 5, pp. 2025-2034, Sept.-Oct. 2010.

[13] B. Axelrod, Y. Berkovich, S. Tapuchi and A. Ioinovici, “Single-Stage Single-Switch Switched-Capacitor Buck/Buck-Boost-Type Converter,” in IEEE Transactions on Aerospace and Electronic Systems, vol. 45, no. 2, pp. 419-430, April 2009.

[14] T. Wu, Y. Lai, J. Hung and Y. Chen, “Boost Converter With Coupled Inductors and Buck–Boost Type of Active Clamp,” in IEEE Transactions on Industrial Electronics, vol. 55, no. 1, pp. 154-162, Jan. 2008.

[15] Y. Zhao, X. Xiang, W. Li, X. He and C. Xia, “Advanced Symmetrical Voltage Quadrupler Rectifiers for High Step-Up and High Output-Voltage Converters,” in IEEE Transactions on Power Electronics, vol. 28, no. 4, pp. 1622-1631, April 2013.

[16] Z. Chen and J. Xu, “High boost ratio DC-DC converter with ripple-free input current,” in Electronics Letters, vol. 50, no. 5, pp. 353-355, 27 Feb. 2014.

[17] W. Li, L. Fan, Y. Zhao, X. He, D. Xu and B. Wu, “High-Step-Up and High-Efficiency Fuel-Cell Power-Generation System With Active-Clamp Flyback–Forward Converter,” in IEEE Transactions on Industrial Electronics, vol. 59, no. 1, pp. 599-610, Jan. 2012.

[18] K. I. Hwu and W. Z. Jiang, “Voltage Gain Enhancement for a Step-Up Converter Constructed by KY and Buck-Boost Converters,” in IEEE Transactions on Industrial Electronics, vol. 61, no. 4, pp. 1758-1768, April 2014.

[19] Q. Luo, Y. Zhang, P. Sun, L. Zhou, “An Active Clamp High Step-Up Boost Converter with a Coupled Inductor,” Journal of Power Electronics, vol. 15, no. 1, pp. 86–95, Jan. 2015.

[20] H. Liu, J. Ai, and F. Li, “A novel high step-up converter with a switched-coupled-inductor-capacitor structure for sustainable energy systems,” Journal of Power Electronics, vol. 16, no. 2, pp. 436–446, Mar. 2016.

[21] Y. P. Siwakoti and F. Blaabjerg, “Single Switch Nonisolated Ultra-Step-Up DC–DC Converter With an Integrated Coupled Inductor for High Boost Applications,” in IEEE Transactions on Power Electronics, vol. 32, no. 11, pp. 8544-8558, Nov. 2017.

[22] B. Gu, J. Dominic, J. S. Lai, Z. Zhao and C. Liu, “High boost ratio hybrid transformer DC-DC converter for photovoltaic module applications,” 2012 Twenty-Seventh Annual IEEE Applied Power Electronics Conference and Exposition (APEC), Orlando, FL, 2012, pp. 598-606.

[23] K. C. Tseng, C. T. Chen, and C. A. Cheng, “A High-Efficiency High Step-Up Interleaved Converter with a Voltage Multiplier for Electric Vehicle Power Management Applications,” Journal of Power Electronics, Vol. 16, No. 2, pp. 414-424, Mar. 2016.

[24] K. Tseng, J. Lin and C. Huang, “High Step-Up Converter With Three-Winding Coupled Inductor for Fuel Cell Energy Source Applications,” in IEEE Transactions on Power Electronics, vol. 30, no. 2, pp. 574-581, Feb. 2015.

[25] L. Yang, T. Liang, H. Lee and J. Chen, “Novel High Step-Up DC–DC Converter With Coupled-Inductor and Voltage-Doubler Circuits,” in IEEE Transactions on Industrial Electronics, vol. 58, no. 9, pp. 4196-4206, Sept. 2011.

[26] S. Saravanan and N. Ramesh Babu, “Analysis and implementation of high step-up DC-DC converter for PV based grid application,” Applied Energy, vol. 190, pp. 64–72, 2017.